

# Black-box optimization and quantum annealing for filtering out mislabeled training instances

Makoto Otsuka<sup>1,2\*</sup>, Kento Kodama<sup>2</sup>, Keisuke Morita<sup>2,3</sup>, and Masayuki Ohzeki<sup>2,3,4</sup>

<sup>1</sup>LiLz Inc., Okinawa, Japan

<sup>2</sup>Graduate School of Information Sciences, Tohoku University, Miyagi, Japan

<sup>3</sup>Sigma-i Co., Ltd., Tokyo, Japan

<sup>4</sup>Department of Physics, Institute of Science Tokyo, Tokyo, Japan

\*m.otsuka@lilz.jp

## ABSTRACT

This study proposes an approach for removing mislabeled instances from contaminated training datasets by combining surrogate model-based black-box optimization (BBO) with postprocessing and quantum annealing. Mislabeled training instances, a common issue in real-world datasets, often degrade model generalization, necessitating robust and efficient noise-removal strategies. The proposed method evaluates filtered training subsets based on validation loss, iteratively refines loss estimates through surrogate model-based BBO with postprocessing, and leverages quantum annealing to efficiently sample diverse training subsets with low validation error. Experiments on a noisy majority bit task demonstrate the method's ability to prioritize the removal of high-risk mislabeled instances. Integrating D-Wave's clique sampler running on a physical quantum annealer achieves faster optimization and higher-quality training subsets compared to OpenJij's simulated quantum annealing sampler or Neal's simulated annealing sampler, offering a scalable framework for enhancing dataset quality. This work highlights the effectiveness of the proposed method for supervised learning tasks, with future directions including its application to unsupervised learning, real-world datasets, and large-scale implementations.

## Introduction

Machine learning is a general framework for extracting underlying patterns contained in data and making accurate predictions or reasonable decisions in new but similar situations based on the learned patterns<sup>1,2</sup>. Although many machine learning models have been proposed for various problem settings, most assume that the given data are correctly annotated and that the given target labels are noise-free. However, the given dataset is often noisy in real-world applications and contains mislabeled instances due to human errors or other unforeseen reasons<sup>3,4</sup>. These mislabeled instances can significantly degrade the generalization performance of the trained model, highlighting the critical need for robust techniques to handle noisy data<sup>5-7</sup>.

Several studies have examined the benefits of data cleansing when faced with contaminated datasets. For example, removing outliers or mislabeled instances before training has improved classification accuracy<sup>5,6</sup>. Moreover, the benefits of eliminating harmful training instances often surpass those of hyperparameter optimization<sup>7</sup>. Previous work has used outlier detection methods, noise removal techniques, or ensembles of different algorithms to eliminate mislabeled instances<sup>8</sup>. Another approach involves removing instances that are mostly misclassified by a set of classifiers<sup>5,7</sup>. Furthermore, some studies indicate that noise in class labels has a greater negative impact on the performance of the induced model than noise in input attributes<sup>9,10</sup>. All of these studies indicate that the removal of detrimental instances significantly improves the quality of the learned model. However, these existing approaches have shown limited success in removing noise from contaminated training datasets due to the inherent challenges of the problem. Specifically, removing mislabeled instances is a combinatorial optimization problem. The number of possible data point combinations increases exponentially with the size of the dataset, making brute-force methods impractical.

To address these challenges, this study proposes an approach to noise removal that combines surrogate model-based black-box optimization (BBO)<sup>11-14</sup> with postprocessing<sup>15</sup> and quantum annealing<sup>16-18</sup>. Quantum annealing is particularly well suited to solve combinatorial optimization problems<sup>19,20</sup>, due to its demonstrated ability to efficiently sample diverse and high-quality solutions<sup>21,22</sup>. By leveraging these strengths, the proposed method identifies and effectively removes mislabeled instances from potentially contaminated training datasets.

Our approach utilizes (1) a concrete validation loss metric for selecting data points under the assumption of a clean validation dataset, (2) a sequential training subset selection strategy utilizing BBO with a surrogate model estimating validation loss, and (3) the unique capabilities of quantum annealers to sample diverse and high-quality solutions efficiently. Together, these components address the challenges of noise removal in a structured and scalable manner.

The remainder of this paper is organized as follows. In the next section, we first describe the noisy majority bit task designed

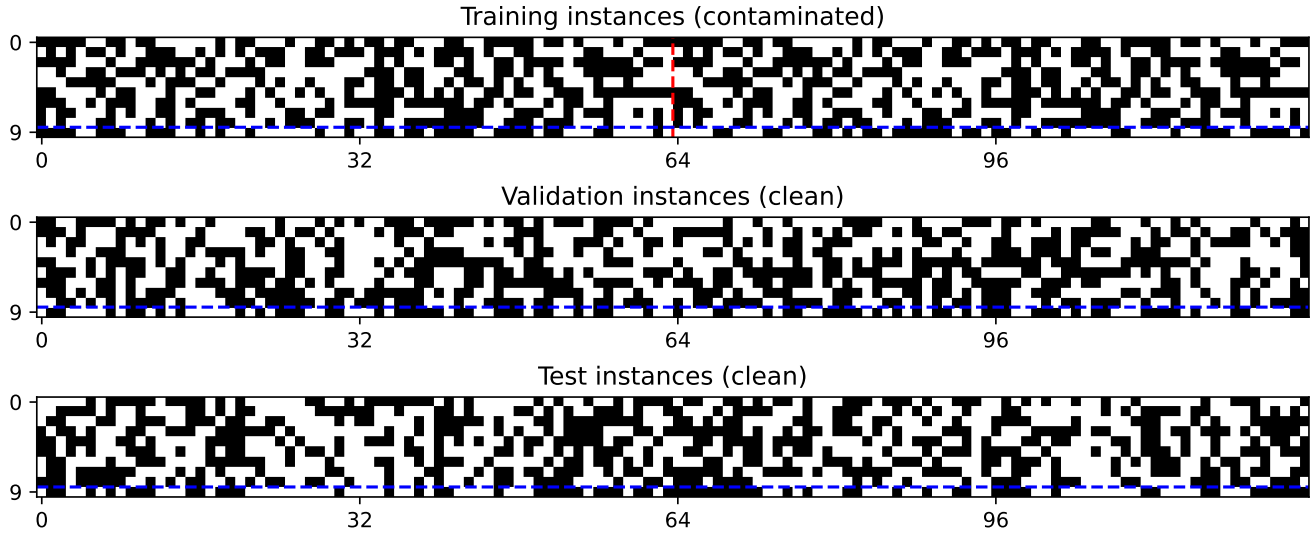


**Figure 1.** Training, validation and test datasets for the noisy majority bit task. For any dataset, each column represents a specific instance composed of 9 input bits  $\mathbf{x} \in \{0, 1\}^9$  and 1 target bit  $t \in \{0, 1\}$ , which are separated by the horizontal dashed blue line. 64, 128, and 128 non-overlapping binary patterns were randomly sampled without repetition to create the input patterns for the training, validation, and test sets, respectively. Each input pattern in the validation and test sets was correctly labeled based on the majority bit of the 9 input bits. The training dataset consists of two halves, separated by a vertical dashed red line. The first half contains 64 real training instances correctly labeled by the majority bits, while the latter half contains 64 fake training instances incorrectly labeled by the minority bits. These incorrectly-labeled fake training instances should be removed for successful training.

to evaluate the proposed method and then explain the proposed method in detail with its two building blocks: the surrogate model-based BBO with postprocessing and energy-based samplers such as D-wave’s quantum annealer. In the following section, we show experimental results with unique characteristics of the proposed method, including prioritized removal of high-risk mislabeled instances, iterative improvement of solution quality, and its ability to leverage D-Wave’s quantum annealer to reach better solutions faster. In the final section, we discuss the insights gained from this study and outline potential directions for future work.

## Methods

### Noisy majority bit task

To evaluate the effectiveness of the proposed algorithm in removing mislabeled instances, we designed a classification task called the noisy majority bit task. This task aims to predict the majority bit in a given binary input vector. The dataset for this task is partitioned into distinct, non-overlapping training, validation, and test sets to ensure an unbiased evaluation. For instance, the correct target label is 0 for the binary input vector  $[0, 0, 0, 1, 0, 1, 0, 0, 1]$ , whereas 1 for  $[1, 1, 0, 1, 0, 1, 1, 0, 0]$ . Under ideal conditions, where all training instances are accurately labeled according to the majority bit, this task would be straightforward. However, the actual training set includes noisy instances where the labels are flipped to the minority bit, introducing mislabeled data. This contamination makes the noisy majority bit task non-trivial, providing a controlled and challenging framework for evaluating the proposed algorithm’s effectiveness in noise removal.

The training, validation, and test sets were constructed as follows. Nine-dimensional input feature vectors for these sets were generated by randomly sampling 64, 128, and 128 unique binary vectors, respectively. All instances in the validation and test sets were correctly labeled according to their majority bits, ensuring clean datasets for evaluation. For the training set, the 64 input vectors were used to create 128 labeled training instances: 64 correctly labeled (*real*) instances with majority-bit labels and 64 mislabeled (*fake*) instances with minority-bit labels. An overview of these datasets, used in all experiments, is shown in Fig. 1.

In this task, the assumption of a clean validation set is critical, as detrimental instances in the training set cannot be identified or removed without the additional information provided by the validation set. Without filtering out the mislabeled training instances, no base model can achieve better-than-chance performance based solely on the contaminated training set. Therefore, the successful removal of mislabeled instances is essential for training a base model that performs effectively on the test set.

By reducing the validation loss against the noise-free validation set, we can remove potentially detrimental training instances from the training dataset. By assuming the correctly-labeled validation dataset, we can use the validation loss as a proxy for the generalization performance of the trained model. In other words, we can evaluate how good the particular training subset is by the validation loss of the model trained on the filtered training subset.

## Surrogate model-based BBO with postprocessing

Although validation loss can be used as a proxy for the generalization performance of a trained model, it is computationally prohibitive to evaluate the validation loss for all possible subsets of the original training dataset. To address this issue, we employed surrogate model-based BBO<sup>11-14</sup> with postprocessing<sup>15</sup> to efficiently identify training subsets with low validation error in an iterative manner. It is important to note that while surrogate model-based BBO with postprocessing is not a novel approach, its application to noise removal and the incorporation of diverse samples obtained from quantum annealer during the sample acceptance process are remarkable contribution of this work. The following part explains the detailed procedure of this algorithm and its application to removal of mislabeled training instances. The pseudo code of the algorithm is shown in Algorithm 1.

---

### Algorithm 1 Mislabeled instance removal algorithm using surrogate model-based BBO with postprocessing

---

**Input:**  $D_{\text{train}} \equiv \{(\mathbf{x}_1, t_1), \dots, (\mathbf{x}_n, t_n)\}, D_{\text{valid}}$ , QUBO-based sampler, Number of samples drawn from the sampler  $M$ , Total number of steps  $N$ ; Number of initialization steps:  $N_0$ , Regression model  $R$ , Supervised-learning model  $P$ , Monotonically increasing function  $g$

**Output:**  $\mathbf{q}_{k^*}$  with the lowest validation loss

```

1: for  $k = 1$  to  $N$  do
2:   if  $k \leq N_0$  then
3:     Randomly sample  $\mathbf{q}_k \in \{0, 1\}^n$ 
4:   else
5:     Compute coefficient  $\tilde{\boldsymbol{\alpha}}_k \in \mathbb{R}^p$  with the regression model:  $\tilde{\boldsymbol{\alpha}}_k = R(\tilde{\mathbf{q}}_{1:k-1}, \mathbf{I}_{1:k-1})$ 
6:     Sample  $\{\mathbf{q}_k^{(m)}\}_{m=1}^M$  from the sampler using the QUBO  $\mathbf{U}(\tilde{\boldsymbol{\alpha}}_k) \in \mathbb{R}^{n \times n}$ 
7:     if all samples in  $\{\mathbf{q}_k^{(m)}\}_{m=1}^M$  is already contained in the evaluated set  $S_{k-1} \equiv \{\mathbf{q}_1, \dots, \mathbf{q}_{k-1}\}$  then
8:       Randomly sample  $\mathbf{q}_k \in \{0, 1\}^n$  not included in the evaluated set  $S_{k-1}$ 
9:     else
10:      Select the sample with the lowest energy in  $\{\mathbf{q}_k^{(m)}\}_{m=1}^M$  as  $\mathbf{q}_k \in \{0, 1\}^n$ 
11:    end if
12:  end if
13:  Create a filtered training subset  $D_{\text{train}}(\mathbf{q}_k)$ 
14:  Train a supervised learning model  $P$  with  $D_{\text{train}}(\mathbf{q}_k)$  to get the trained model  $P^*$ 
15:  Evaluate the trained model  $P^*$  with  $D_{\text{valid}}$  to get the validation loss  $L_{\text{valid}}(\mathbf{q}_k)$ 
16:  Compute  $l_k = g(L_{\text{valid}}(\mathbf{q}_k))$  where  $g$  is a monotonically increasing function
17:  Keep  $\mathbf{q}_k \in \{0, 1\}^n$  as an evaluated set  $S_k \equiv \{\mathbf{q}_1, \dots, \mathbf{q}_k\}$ 
18:  Keep  $\tilde{\mathbf{q}}_k \in \{0, 1\}^p$  as a matrix  $\tilde{\mathbf{q}}_{1:k} \in \{0, 1\}^{k \times p}$ 
19:  Keep  $l_k \in \mathbb{R}$  as a vector  $\mathbf{l}_{1:k} \in \mathbb{R}^k$ 
20: end for

```

---

First, let us denote the training, validation, and test sets as  $D_{\text{train}}$ ,  $D_{\text{valid}}$ , and  $D_{\text{test}}$ , respectively. The potentially contaminated original training dataset is defined as  $D_{\text{train}} \equiv \{(\mathbf{x}_i, t_i)\}_{i=1}^n \equiv \{(\mathbf{x}_1, t_1), \dots, (\mathbf{x}_n, t_n)\}$  where the  $i$ -th tuple  $(\mathbf{x}_i, t_i)$  is called the  $i$ -th training instance, which is defined as a pair of  $i$ -th input feature vector  $\mathbf{x}_i$  and  $i$ -th target label  $t_i$ . Target labels are assumed to be noisy in  $D_{\text{train}}$  but noise-free in both  $D_{\text{valid}}$  and  $D_{\text{test}}$ .

Second, let us define an  $n$ -dimensional binary selection vector  $\mathbf{q} \in \{0, 1\}^n$  to denote a filtered training subset  $D_{\text{train}}(\mathbf{q}) \subseteq D_{\text{train}}$ . The  $i$ -th training instance  $(\mathbf{x}_i, t_i) \in D_{\text{train}}$  is included in a filtered training subset  $D_{\text{train}}(\mathbf{q}) \subseteq D_{\text{train}}$  if  $q_i = 1$  and excluded if  $q_i = 0$ . Thus, a binary pattern  $\mathbf{q}$  uniquely determines a specific filtered subset  $D_{\text{train}}(\mathbf{q})$  from the original training dataset  $D_{\text{train}}$ . Consequently, there are  $2^n$  possible realizations of filtered training subsets  $D_{\text{train}}(\mathbf{q})$  in total.

Third, we introduce the surrogate model  $f_{\tilde{\alpha}}(\mathbf{q})$ , which is defined as

$$f_{\tilde{\alpha}}(\mathbf{q}) = \alpha_0 + \mathbf{q}^\top \mathbf{U}(\tilde{\alpha}_{\setminus 0}) \mathbf{q} \quad (1)$$

$$= \alpha_0 + \mathbf{q}^\top \begin{bmatrix} \alpha_1 & \alpha_{1,2} & \cdots & \alpha_{1,n} \\ 0 & \alpha_2 & \cdots & \alpha_{2,n} \\ \vdots & \vdots & \ddots & \vdots \\ 0 & 0 & \cdots & \alpha_n \end{bmatrix} \mathbf{q} \quad (2)$$

$$= \alpha_0 + \sum_j \alpha_j q_j + \sum_{i < j} \alpha_{i,j} q_i q_j \quad (3)$$

$$= [\alpha_0, \alpha_1, \dots, \alpha_n, \alpha_{1,2}, \alpha_{1,3}, \dots, \alpha_{n-1,n}] [1, q_1, \dots, q_n, q_1 q_2, q_1 q_3, \dots, q_{n-1} q_n]^\top \quad (4)$$

$$= \tilde{\alpha}^\top \tilde{\mathbf{q}} \quad (5)$$

to estimate the validation loss of the the model trained by the filtered training subset  $D_{\text{train}}(\mathbf{q})$ . In the surrogate model-based BBO, the surrogate model plays two roles: one is to approximate the unknown cost function with a quadratic binary form and the other is to generate binary samples with sufficiently low cost values. Here, the surrogate model  $f_{\tilde{\alpha}}(\mathbf{q})$  is parameterized by the parameter vector  $\tilde{\alpha} \in \mathbb{R}^p$  given in the form of Eq. (4) where  $p = 1 + n + n(n-1)/2$ . The elements in this parameter vector  $\tilde{\alpha}$  are also found in the constant-shifted quadratic unconstrained binary optimization (QUBO) form in Eq. (2). Eq. (2) is composed of the first term  $\alpha_0$  which represents a constant shift and the second quadratic term which represents linear interaction by its diagonal elements and pair-wise interaction by its off-diagonal elements. In short, the unknown true cost function  $f(\mathbf{q})$  over  $\mathbf{q} \in \{0, 1\}^n$  is approximated by the second order Taylor expansion around  $\mathbf{q}$ , which is  $f_{\tilde{\alpha}}(\mathbf{q})$  in the form shown in Eq. (3). The quality of this approximation can be improved by adjusting the parameter vector  $\tilde{\alpha}$ .

Fourth, we sample low-cost binary patterns  $\mathbf{q}$  from the constant-shifted surrogate model  $f_{\tilde{\alpha}}(\mathbf{q}) - \alpha_0$ , which takes the quadratic form as shown in Eq. (1) and we can use any QUBO-based sampler such as a sampler running on D-Wave System's quantum annealer. The sampler generates a binary pattern  $\mathbf{q}$  with sufficiently low cost value  $f_{\tilde{\alpha}}(\mathbf{q})$  under the fixed parameter vector  $\tilde{\alpha}$ .  $M$  samples are drawn simultaneously from a sampler in a single sampling step.

Fifth, we update the parameter vector  $\tilde{\alpha}$  to minimize the validation loss of the model trained by the filtered training subset  $D_{\text{train}}(\mathbf{q})$ . This optimization can be done in two phases. The first phase updates the parameter vector  $\tilde{\alpha}$  using the random samples in a batch manner. The second phase updates the parameter vector  $\tilde{\alpha}$  in an online manner using all samples accepted up to the current step.

In the first phase, we randomly samples the  $n$ -dimensional binary pattern  $\mathbf{q}_k \in \{0, 1\}^n$  sequentially from  $k = 1$  to  $k = N_0$ , and then for each binary pattern  $\mathbf{q}_k$ , we compute the validation loss  $L_{\text{valid}}(\mathbf{q}_k)$  of the model trained by the filtered training subsets  $D_{\text{train}}(\mathbf{q}_k)$ . The validation loss  $L_{\text{valid}}(\mathbf{q}_k)$  might not be distributed normally, and it is often preferable to transform it by a monotonically increasing function  $g$  such as the log function to make it more normally distributed when this value becomes the target of some model and this is the case in our algorithm. Let us define the transformed validation loss as  $l_k = g(L_{\text{valid}}(\mathbf{q}_k))$ . If we define  $\tilde{\mathbf{q}}$  as in Eq. (4), the transformed validation loss  $l_k$  can be approximated by the surrogate model  $f_{\tilde{\alpha}}(\mathbf{q}_k)$  in the form of Eq. (5), which is linear in  $\tilde{\mathbf{q}}$ . Therefore, if we collect the transformed validation losses  $\{l_1, \dots, l_{N_0}\}$  and the corresponding binary patterns  $\{\mathbf{q}_1, \dots, \mathbf{q}_{N_0}\}$ , we can update the parameter vector  $\tilde{\alpha}$  to minimize the transformed validation losses  $\{l_1, \dots, l_{N_0}\}$ . This optimization can be done in many forms such as the Bayesian linear regression with sparse prior<sup>11,23,24</sup>, the LASSO regression<sup>25</sup>, and the Ridge regression to update the parameter vector  $\tilde{\alpha}$  depending on the sparsity assumption of the given problem. This first step is necessary to obtain a good initial guess of the parameter vector  $\tilde{\alpha}$ .

In the second phase, we sequentially accept one good sample per step and compute the parameter vector  $\tilde{\alpha}_k$  with sequentially updated input-output pairs  $\{(\tilde{\mathbf{q}}_j, l_j)\}_{j=1}^{k-1}$  available at each time step  $k \in \{N_0 + 1, N_0 + 2, \dots, N\}$ . The good sample is selected as follows. After drawing  $M$  samples  $\{\mathbf{q}_k^{(m)}\}_{m=1}^M$  from a sampler at step  $k$ , the one with the lowest energy that is not included in the accepted sample set  $S_{k-1} \equiv \{\mathbf{q}_1, \dots, \mathbf{q}_{k-1}\}$  is selected. If no such sample exists, a random sampling is conducted until a previously unseen sample is found, which is then accepted. The accepted sample  $\mathbf{q}_k$  at step  $k$  is then used to compute the transformed validation loss  $l_k$  at step  $k$ , by transforming the validation loss  $L_{\text{valid}}(\mathbf{q}_k)$  of the model trained by a filter training subset  $D_{\text{train}}(\mathbf{q}_k)$ . Newly obtained quantities at time step  $k$  such as  $\mathbf{q}_k \in \{0, 1\}^n$ ,  $\tilde{\mathbf{q}}_k \in \{0, 1\}^p$ ,  $l_k \in \mathbb{R}$  are stored for the next iteration. At the end of the second phase, the best sample  $q_{k^*}$  with the lowest transformed validation cost is reported where  $k^* = \text{argmin}_k l_k$ .

In our experiment, we used the following parameters and settings.  $n = 128$ ,  $N_0 = 64$ ,  $N = 320 (= 64 + 256)$ ,  $M = 512$ ,  $p = 8257 = 1 + 128 + 128 \times (128 - 1)/2$ . We used a logistic regression model as a task-specific base model for solving the noisy majority bit task. The reason for using this model is that it is simple, interpretable, and fast to train. As a linear model for estimating  $\tilde{\alpha}$ , we used the ridge regression model instead of the Bayesian model with sparsity prior or the Lasso model, which is usually used in the context of the surrogate model-based BBO to impose the sparsity constraint on the QUBO matrix. The

reason for not using sparse-version of the model is that the data is generated in such a way that half of the training data points have noisy labels, and we expect the resulting QUBO matrix can be well approximated without sparsity assumption.

### D-Wave’s quantum annealer and related samplers

Due to the combinatorial nature of the problem, it is difficult to find the optimal solution in a reasonable amount of time. To address this issue, we propose to leverage the characteristics of D-Wave Systems’ quantum annealer, which is known to provide near-optimal and diverse samples quickly<sup>21,22</sup>.

We used three samplers in this study. The first sampler is the OpenJij’s simulated quantum annealing (SQA) sampler, which is a classical sampler provided by the private company called Jij<sup>26</sup>. The second sampler is the Neal’s simulated annealing (SA) sampler, another classical sampler offered by D-Wave Systems<sup>27</sup>. We selected Neal’s SA sampler over OpenJij because of their comparable performance characteristics<sup>28</sup>, thereby ensuring a fair comparison with the subsequent sampler also offered by D-Wave Systems. The third sampler is the D-Wave’s clique sampler<sup>29</sup>, running on the physical quantum annealer called the D-Wave Advantage 6.4<sup>30</sup>. In the following section, we will refer to these samplers as the OpenJij SQA sampler, the Neal SA sampler, and D-Wave QA clique sampler, respectively.

For all three samplers, we used the latest version of the respective Python packages available at the time and employed their default parameters for class instantiation without modifications unless otherwise specified. For the OpenJij SQA sampler, we used the `openjij.SQASampler` class from the `openjij` package (version 0.9.2). For the Neal SA sampler, we employed the `neal.SimulatedAnnealingSampler` class from the `dwave-neal` package (version 0.6.0). For the D-Wave QA clique sampler, we utilized the `dwave.system.samplers.DWaveCliqueSampler` class from the `dwave-sampler` package (version 1.2.0) with D-Wave’s Advantage system 6.4 as its solver. For all samplers, the `num_reads` parameter was set to 512, and for both OpenJij SQA and Neal SA samplers, the default `num_sweeps` value of 1000 was employed. All experiments were conducted on a MacBook Pro 2023 equipped with Apple M2 Max processor and 96 GB of memory.

## Results

### Prioritized removal of high-risk mislabeled instances

As illustrated in Fig. 2, our proposed algorithm coupled with any of three samplers consistently removed mislabeled instances (located to the right of the dotted red line in the figure) from the contaminated original training dataset, while preserving the correctly labeled ones (shown to the left of the dotted red line in the figure). For any sampler, the subset of removed instances differed with each run, but their selection patterns remained consistent across runs. The D-Wave QA clique sampler and the Neal SA sampler consistently kept correctly labeled instances in higher probability than the OpenJij SQA sampler. However, regardless of this sampler-dependent performance difference in noise removal, the proposed algorithm appears to work well in removing mislabeled instances from the contaminated training dataset.

A logistic regression model trained on the cleansed training dataset consistently demonstrated improved performance across all 32 runs as shown in Fig. 3. Here, we focus on analyzing the results obtained using the D-Wave QA clique sampler, as similar conclusions are likely applicable to the other samplers. The training errors computed on the optimized training subsets were consistently lower than the training errors computed on the original training sets without noise removal. This indicates that the mislabeled instances were successfully filtered out from the contaminated training dataset. Regardless of successful removal of the mislabeled instances, the training errors computed on the filtered training subsets remained consistently higher than the validation and test errors. This discrepancy arises because some mislabeled instances persist in in the filtered dataset even after noise removal by the proposed algorithm. Please note that the validation error is lowest because it is used as the objective function of the surrogate model-based BBO, and all instances in the validation dataset are noise free. The low test errors suggest that the proposed algorithm effectively removed mislabeled instances in a way to guarantee the generalization of the trained model.

Further analysis revealed that mislabeled instances with a greater negative impact if not removed are more likely to be eliminated in an input-feature-dependent fashion. Fig. 2 shows that the difference in removal probabilities of fake instances are persistent over different runs and different samplers. In other words, there is a pattern in removal probability of fake instances. Fig. 4 shows the 64 input vectors contained in the fake training instances and their characteristics, such as the summed value of each input vector, together with their removal probabilities computed after 32 runs with the D-Wave QA clique sampler. The relationship between the summed values of input patterns and the removal probabilities of their associated instances is shown in Fig. 5(a). Specifically, the summed input pattern,  $s_i = \sum_{c=1}^9 x_{i,c}$ , or equivalently the probability of an element of the input vector taking the value of 1,  $p_i = s_i/9$ , is shown to influence the removal probability of the input pattern  $\mathbf{x}_i \in \{0, 1\}^9$ . To clarify this relationship, Fig 5(b) presents the absolute deviance of summed input pattern from the optimal threshold of 4.5, which is optimal for solving the majority bit task. This absolute deviance defined as  $d(\mathbf{x}_i) = |9p_i - 4.5|$  is computed for 64 unique input patterns in the training set  $\{\mathbf{x}_i\}_{i=1}^{64}$ . Notably, this absolute deviance is inversely related to the entropy of a binary input pattern, defined as  $s(\mathbf{x}_i) = -p_i \log p_i - (1 - p_i) \log(1 - p_i)$ . Therefore, Fig 5(b) demonstrates that mislabeled input patterns with lower

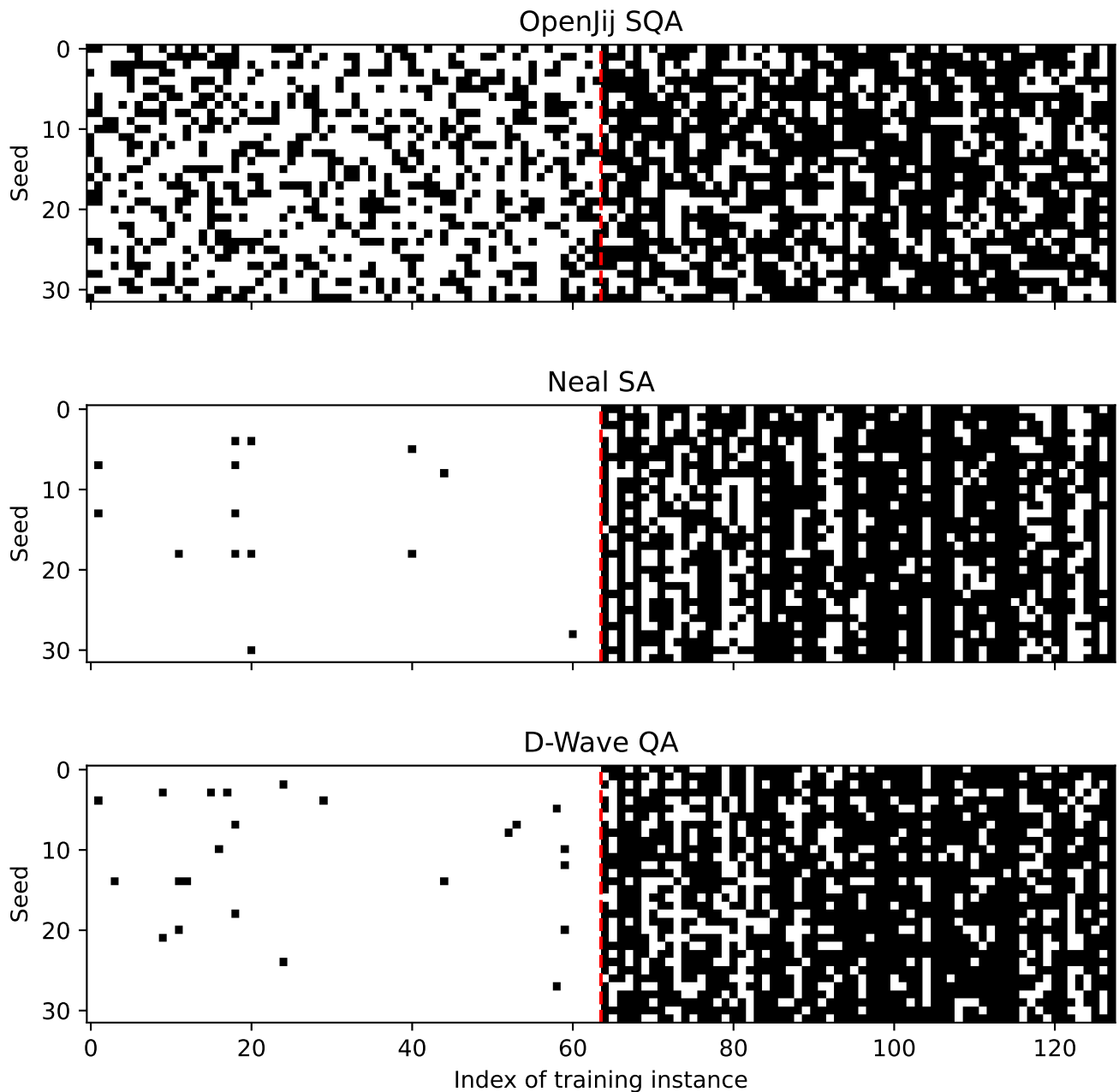


**Figure 2.** Instance removal patterns acquired by three different samplers over 32 runs. Each cell in the grid represents the inclusion or exclusion status of a training instance for a specific run. For any sampler, a white cell at the  $r$ -th row and  $i$ -th column indicates the  $i$ -th training instance is included in the filtered training set and used for actual training in the  $r$ -th run. The black cell, on the other hand, shows the same training instance is excluded from the filtered training set and not used for training in the associated run. Seed values are changed from 0 to 31 to see how consistently the proposed algorithm coupled with a certain sampler filters out mislabeled training instances and retains correctly labeled training instances.

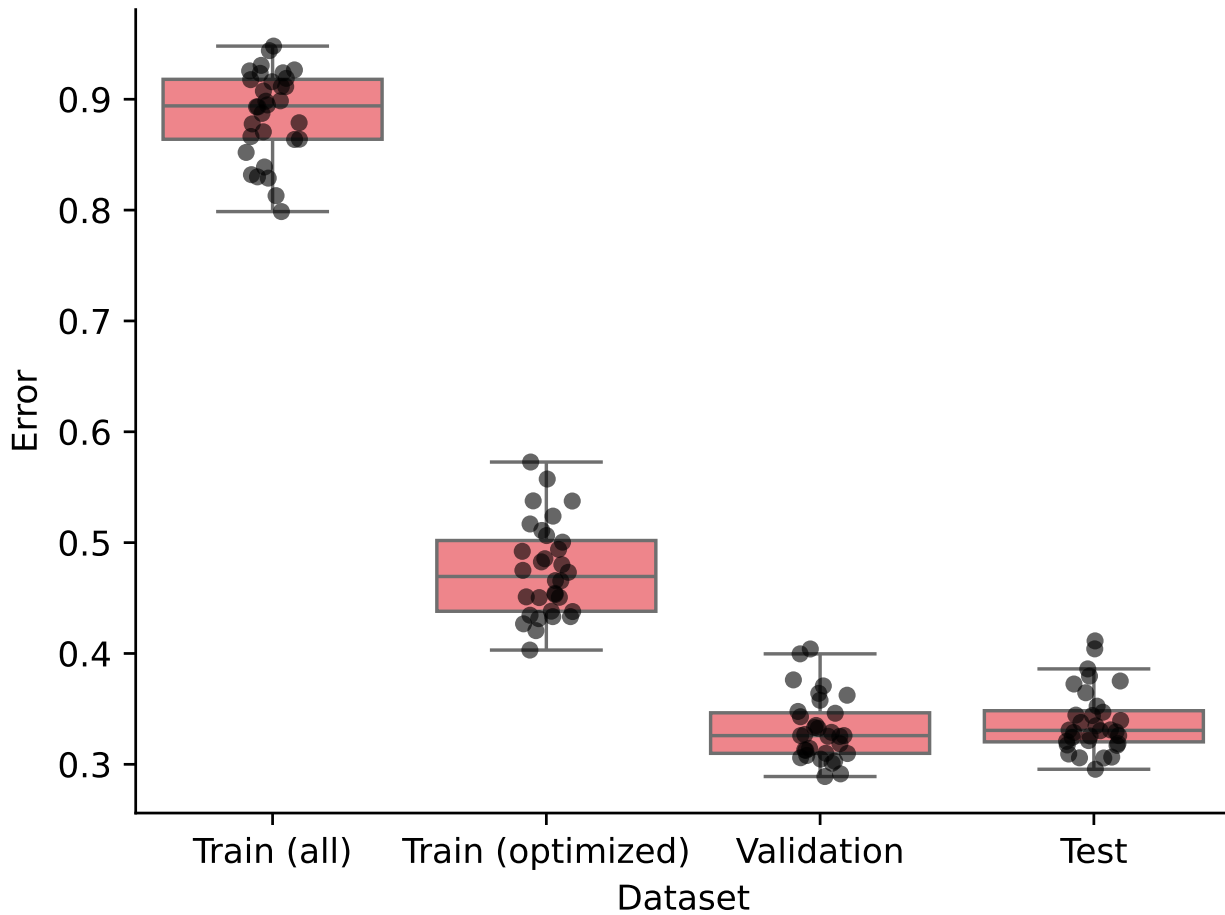


**Figure 3.** Performance of the trained model on four different datasets. In each run, a model was trained using a filtered training dataset and then evaluated on four different datasets. The model performance was measured in log-loss error metric. Each gray dot represents one of the 32 log-loss errors for a specific dataset. Variations in error values within the same dataset are due to differences in the training instances selected across different runs by our dataset optimization algorithm. The labels *Train (all)* and *Train (optimized)* indicate whether all or filtered instances in the training dataset were used for model evaluation, respectively. The whiskers extend to the farthest points within 1.5 times the inter-quartile range from the nearest hinge of the box plot.



entropy, which correspond to higher absolute deviance, are more likely to be removed. This trend may be attributed to the stronger negative impact of low-entropy patterns with incorrect labels (e.g.,  $[0, 0, 0, 0, 0, 0, 0, 0]$  labeled as 1) on the trained model, compared to high-entropy patterns with incorrect labels (e.g.,  $[0, 1, 0, 1, 0, 1, 0, 1, 0]$  labeled as 1).

### Iterative improvement of solution quality

Now let us shift our attention to compare the difference between three samplers: OpenJij SQA sampler, Neal SA sampler, and D-Wave QA clique sampler. As shown in Fig. 6, in this particular run, the D-Wave QA clique sampler attained the lowest loss value followed by Neal SA and the OpenJij SQA samplers. This tendency is not always true in different runs as shown in Fig. 7, but D-Wave QA clique sampler successfully found multiple solutions better than the best solution found in 32 runs of the Neal SA sampler in terms of surrogate loss (Fig. 7(a)) and Hamming distance between the theoretical solution and the found solutions (Fig. 7(b)).

Fig. 6 also shows the interesting difference in how 512 samples are utilized by each sampler in each optimization step. Firstly, in case of OpenJij SQA sampler, the optimal sample with lowest energy in 512 samples is always accepted in each optimization step. This is due to the fact that both the variance and the mean of energy distribution of samples obtained by OpenJij SQA sampler is always higher than ones obtained by Neal SA sampler or D-Wave QA clique sampler as shown in Fig. 8. Secondly, in case of Neal SA sampler, most of 512 samples obtained in each step are the same and have equal energy as shown in Fig. 8(b) (In this particular run, they are all equal). Therefore, there is a higher chance for the optimal sample in a certain step to be already seen before, and it cause the higher chance of random samples to be selected (See the higher probability of random samples marked by black cross shown in Fig. 6(b)). Thirdly, in the case of D-Wave QA clique sampler, suboptimal sample with sufficiently low energy is fully utilized to find lower energy solution in each optimization step as shown in Fig. 6(c).

### Leveraging D-Wave’s quantum annealer to reach better solutions faster

As shown in Fig. 8(c), 512 samples obtained by D-Wave QA clique sampler in each step have higher variety compared to ones obtained by Neal SA sampler shown in Fig. 8(b). This variety in 512 samples increases as the optimization phase proceeds as shown in Fig. 8(c). Notice toward the end of optimization phase, the number of accepted random samples is gradually reduced as shown in Fig. 6(c).

In addition to achieving high solution quality, the D-Wave QA clique sampler demonstrated significantly faster sampling time compared to other samplers when using the default parameter settings. Sampling time of D-Wave QA clique sampler is about 10 times faster than one of Neal SA sampler and is about 100 times faster than one of OpenJij SQA sampler as shown in Fig. 9.

## Discussion and Conclusion

The proposed algorithm successfully identified mislabeled instances contained in the contaminated training dataset as shown in the previous section. Because our task is designed to be impossible to solve above the chance level without proper identification of mislabeled instances, the successful improvement in the generalization performance of the trained model, which is reflected in the test error, indicates that the proposed algorithm is proved to be effective in identifying mislabeled instances. Our approach to the problem of removing mislabeled instances became possible by combining the surrogate model-based BBO and quantum annealer with clearly defined loss function using noise-free validation dataset.

We have obtained several important insights from the results. First, we have observed that the proposed algorithm removed mislabeled instances that have more detrimental effect on the model’s generalization performance with higher probability. This favorable tendency likely arises from leveraging the validation error—directly tied to generalization performance—as the objective function in the surrogate model-based BBO. In our task, mislabeled instances with lower input entropy tend to exert a stronger negative influence on generalization performance and are therefore more likely to be removed. This suggests that the proposed algorithm inherently possesses the capability to prioritize the removal of mislabeled instances that exert a more detrimental impact on the generalization ability of the trained model. Therefore, the proposed algorithm is also likely be effective for removing mislabeled instances with complex input features such as images or texts. Second, we have observed that the proposed algorithm effectively leveraged the sample diversity provided by the quantum annealer, driven in part by quantum fluctuations, to achieve a lower validation loss. Quantum annealers are capable of generating diverse solutions rapidly due to their inherent quantum fluctuations, which facilitates exploration of the solution space. As a result, the combination of the quantum annealer and the surrogate model-based BBO may prove valuable for addressing combinatorial optimization problems with a vast solution space, extending beyond noise removal to other problem setups.

The proposed algorithm has multiple future directions to explore. Here in this study, we have focused on the problem of discarding unimportant instances from a given dataset. However, we can easily extend the proposed algorithm to simultaneously discard unimportant features as well as instances by allocating binary nodes over features as well as instances. It is of course



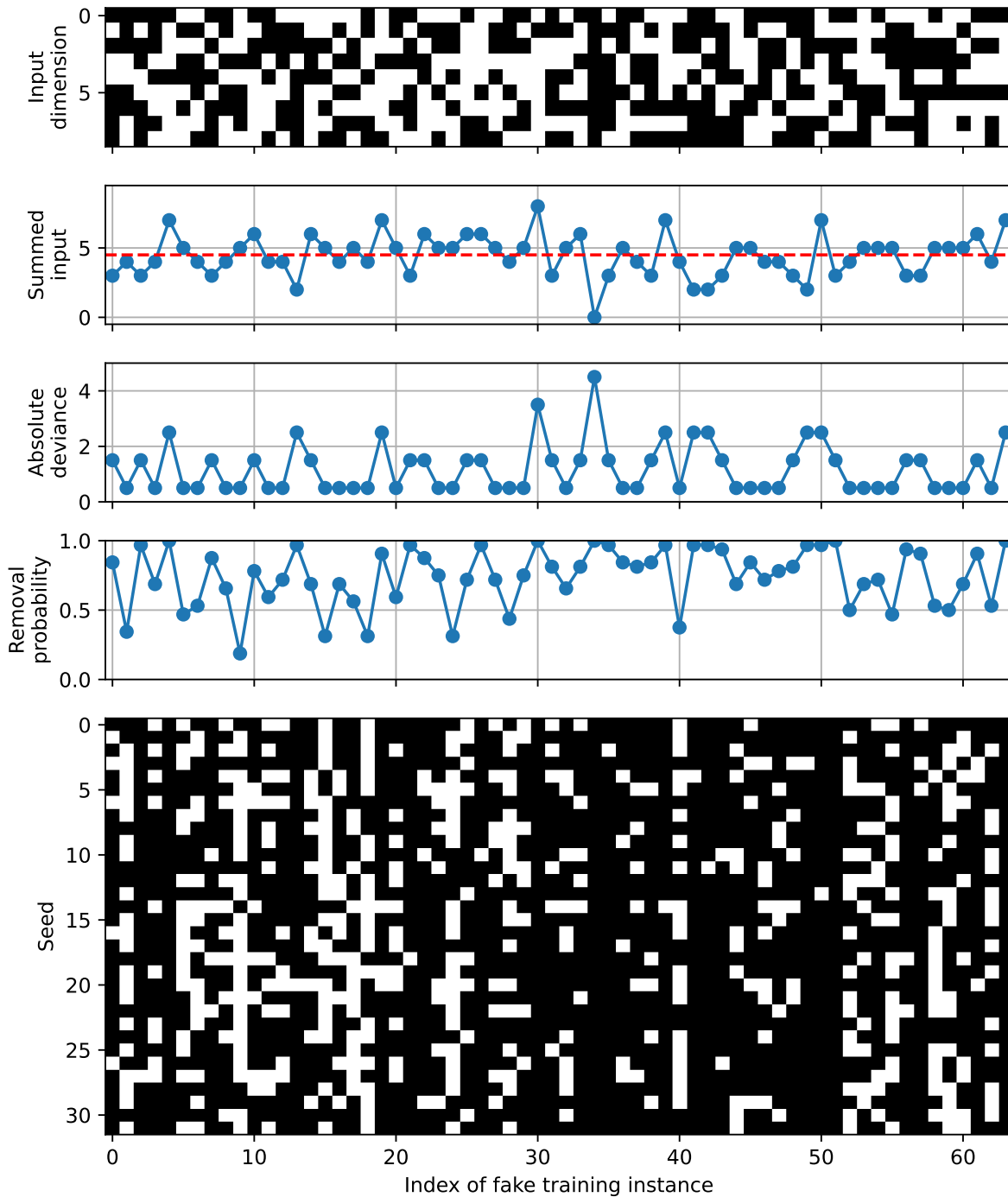


**Figure 4.** Characteristics of the input patterns of the fake training instances and their removal probabilities using the D-Wave QA clique sampler. 1) The 9 dimensional binary input patterns of the fake training instances. 2) The summed values of input patterns, with the horizontal dashed red line marking the optimal decision boundary of 4.5. 3) The absolute deviance (or distance) of summed input patterns from the optimal decision boundary of 4.5. 4) The removal probabilities of incorrectly labeled fake instances over 32 runs with different seed values ranging from 0 to 31. 5) The removal patterns of fake training instances across 32 different runs. This removal pattern is also depicted on the right side of the dashed red line in the D-Wave QA clique result shown in Fig. 2.

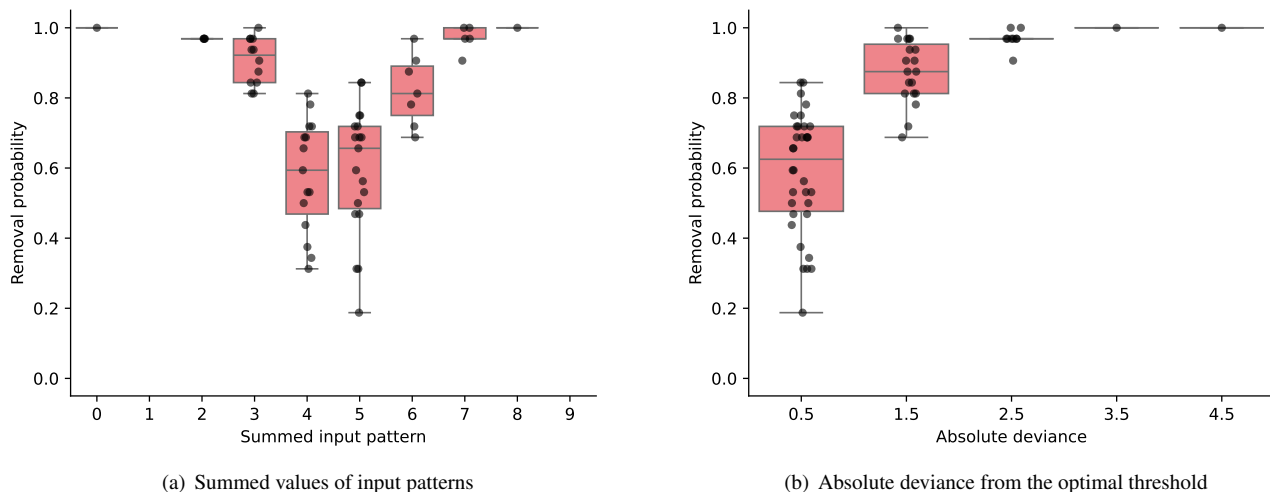


**Figure 5.** Relationship between the removal probabilities and the characteristics of 64 input patterns of the fake training subset. The removal probabilities are compared with (a) the number of ones in each input pattern of the fake training subset and (b) the absolute deviation from the optimal threshold of 4.5 to the summed values of input patterns. In both plots, the whiskers are drawn to the farthest points within 1.5 times the inter-quartile range from the nearest hinge of the box plot.

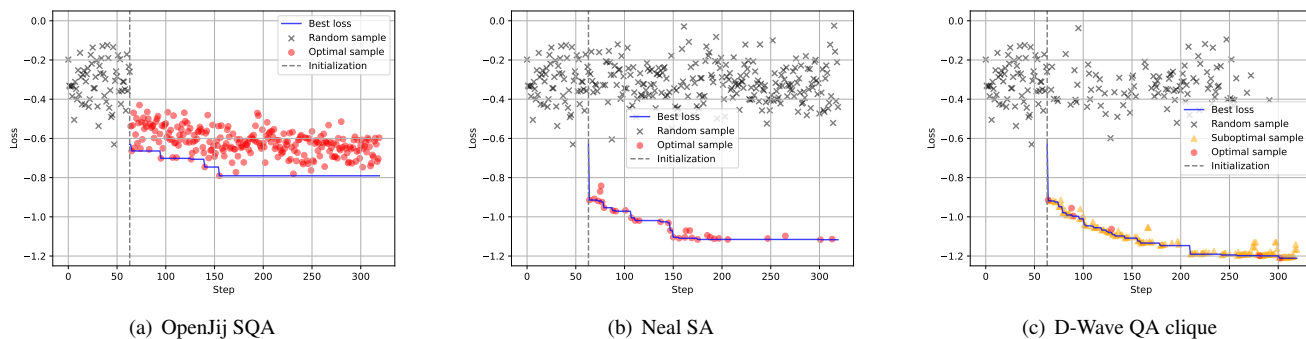
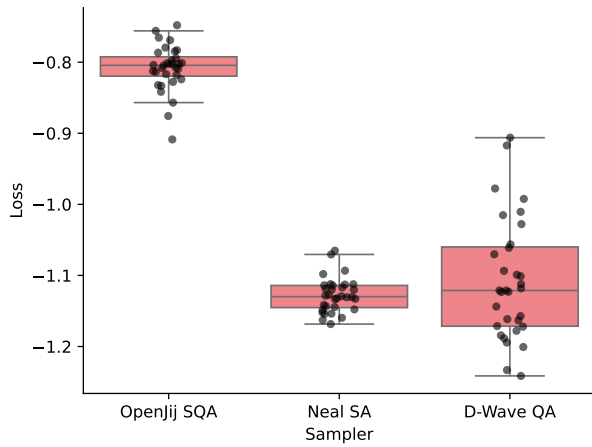
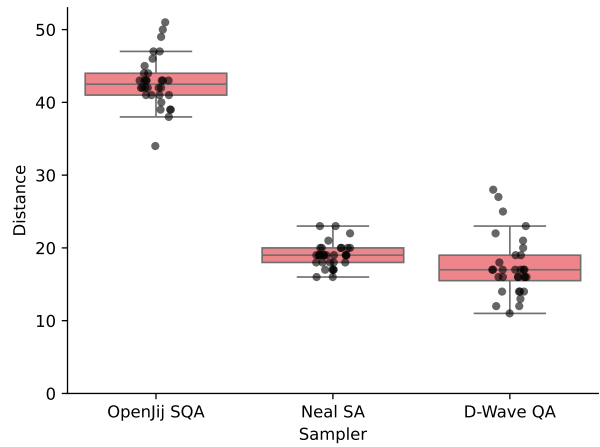


**Figure 6.** Comparison of three samplers in terms of surrogate losses and types of sequentially obtained samples. The first 64 steps up to the dotted gray line are called the initialization phase, during which samples are obtained randomly. The remaining 256 steps constitute the optimization phase, where samples are obtained using the surrogate model-based BBO with postprocessing. In each optimization step, 512 samples are drawn from a selected sampler. These samples are sequentially checked from the one with the lowest energy to the one with the highest energy to see if they are already contained in the accepted sample set. The first sample not contained in the accepted sample set is accepted and inserted into the accepted sample set. If all 512 samples are already contained in the accepted sample set, a new sample not contained in the acquired sample set is drawn randomly. The trend of the lowest energy up to that step is shown with a blue solid line. A sample type is marked as *optimal* if the accepted sample has the lowest energy among the 512 samples. A sample type is marked as *suboptimal* if it is from the 512 samples but does not have the lowest energy. A sample type is marked as *random* if it is not obtained from the 512 samples and is drawn randomly. In all three cases, all parameters are fixed except for the solver types.

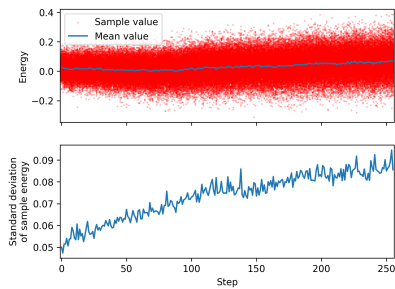


(a) Loss values of the found solutions.

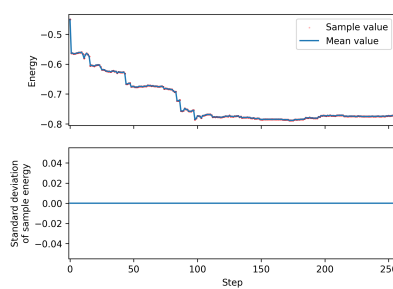


(b) Hamming distances between the theoretical solution and the found solutions.

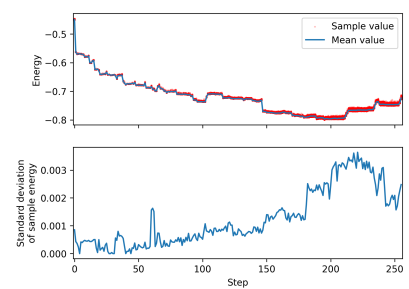
**Figure 7.** Characteristics of the solutions found by each sampler in 32 runs. (a) The loss value of the best solution found by each sampler in each run is represented as a single point. Its distribution over 32 runs is shown as a box plot for each sampler. The whiskers extend to the farthest points within 1.5 times the inter-quartile range from the nearest hinge of the box plot. (b) Hamming distance between the theoretical solution and the best solution found by each sampler in each run is shown in the same format.



(a) OpenJij SQA



(b) Neal SA



(c) D-Wave QA clique

**Figure 8.** Energy distribution of 512 samples obtained in each optimization step of three different samplers: (a) OpenJij SQA sampler, (b) Neal SA sampler, and (c) D-Wave QA clique sampler. The top figure for each sampler shows the raw energy values of 512 samples obtained in each step over the entire 256 steps in the optimization phase. The mean energy value of 512 samples acquired in each step is shown with the blue line. The bottom figure for each sampler shows the standard deviation of the energy values of 512 samples acquired in each step. Please note the energy scales of Neal SA sampler and D-Wave QA clique sampler are the same but different from the one used for the OpenJij SQA sampler.

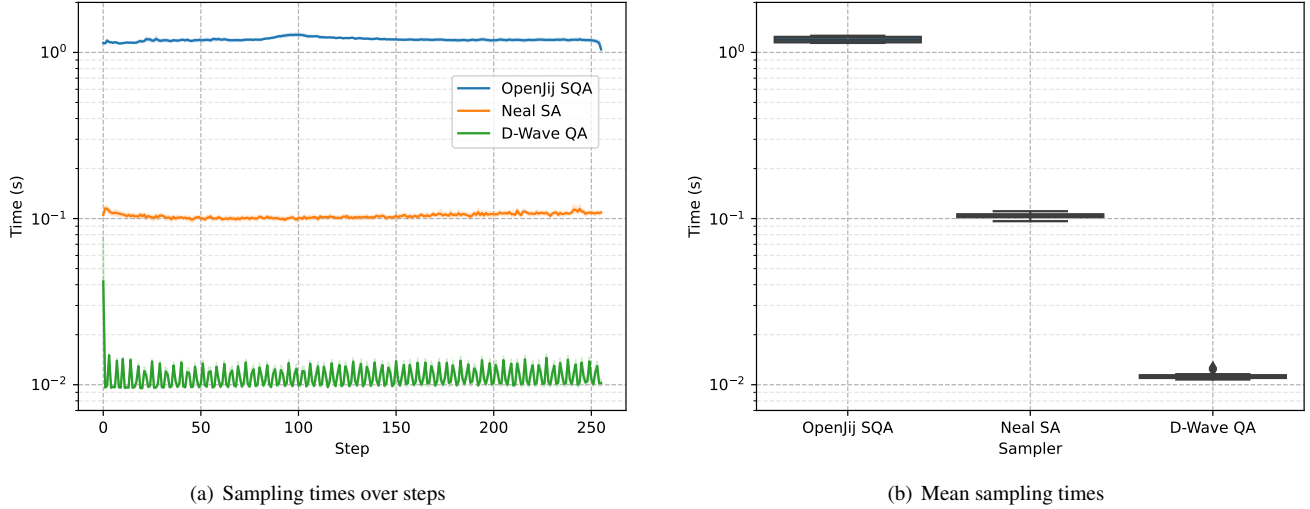


**Figure 9.** Sampling time statistics of three samplers. (a) Sampling times in each step are compared for the three samplers. The 95% confidence intervals obtained after running 32 runs are shown with transparent bands around the mean line plots. (b) The standard error of the mean over 32 runs, where the mean is taken over 256 steps of sampler’s sampling times. The whiskers extend to the farthest points within 1.5 times the inter-quartile range from the nearest hinge of the box plot.

possible to use the proposed method just for feature selection by allocating binary nodes only over features. The objective function remains the same, and we can automatically find relevant features for building the model with high generalization performance. This is the first interesting future direction to explore. Another interesting future direction is to evaluate the proposed algorithm on real-world datasets. In this study, we have only evaluated the proposed algorithm on synthetic datasets to show the effectiveness of the proposed algorithm for removing mislabeled dataset in the hardest case. However, it is important to evaluate the proposed algorithm on real-world datasets to investigate the effectiveness of the proposed algorithm in practical applications. The real world datasets contains different degrees of noises in labels and attributes, and it is important to evaluate how effective the proposed algorithm on these real-world datasets. Also, we used a linear regression model as a base model in this study, but any kind of machine learning models can be used as a base model. Due to the iterative nature of the proposed algorithm, not just sampling time but also the training time of the base model becomes important issue when handing real-world datasets. Therefore, it is important to see how much performance improvement in terms of generalization can be achieved by the proposed algorithm, given the fixed real-world datasets at hand. Yet another interesting future direction is to apply the proposed algorithm to unsupervised learning problems. In this study, we have mainly focused on the supervised learning problem aimed at removing mislabeled instances from a given dataset. However, the proposed algorithm can be also applied to unsupervised learning settings by estimating the suitable objective function such as negative log-partition function of unlabeled observations by the surrogate model. The proposed algorithm is likely to be used to remove unimportant instances or features in the dataset in unsupervised learning settings.

Although the proposed algorithm has shown promising results in a well-controlled setting, there are several limitations in this study. First limitation comes from the fact that the task is artificially created and relatively small in its size. The task is designed to be simple enough to be solved by the logistic regression model, and the number of data points is 128, which is not that large in usual machine learning setting where the simple MNIST dataset has 60,000 training data points. Second limitation comes from the fact that we used the logistic regression model with  $L_2$  regularization as a base model. This choice comes from our prior knowledge for the noisy majority bit task, but it is possible that the LASSO model, which can automatically select important features, might be more suitable for many real-world applications. Third limitation comes from the fact that we have not evaluated the proposed algorithm on large-scale datasets. The proposed algorithm has shown promising results in the noisy majority bit task with 128 instances, but it is possible that the proposed algorithm might not work well on large-scale datasets. Finally, the proposed algorithm is limited by the number of qubits in the quantum annealer. So, if the number of data points exceeds the number of qubits in the quantum annealer, the problem cannot be embedded into the quantum annealer, and the proposed algorithm cannot be applied to the problem.

In this study, we have proposed a novel algorithm capable of removing mislabeled instances from a given training dataset. This algorithm estimates the loss against a correctly-labeled validation dataset using surrogate model-based BBO followed by postprocessing. Additionally, we have demonstrated that the proposed algorithm can be further enhanced in both solution

quality and sampling speed by leveraging the unique characteristics of D-Wave Systems' quantum annealer, such as its sampling diversity and rapid sampling capability. The proposed algorithm provides a new direction for improving the quality of training datasets by combining the power of BBO and quantum annealing. This combination offers a promising approach to tackling the long-standing challenge of data quality improvement. In the future, it is important to evaluate the proposed algorithm on real-world datasets to assess its effectiveness in practical applications. This evaluation will help determine the tangible benefits and potential limitations of the algorithm when applied to complex and diverse data scenarios.

## References

1. Bishop, C. M. *Pattern Recognition and Machine Learning* (Springer, 2006).
2. Murphy, K. P. *Machine Learning: A Probabilistic Perspective* (MIT press, 2012).
3. Lee, G. Y., Alzamil, L., Doskenov, B. & Termehchy, A. A survey on data cleaning methods for improved machine learning model performance. *arXiv preprint arXiv:2109.07127* (2021). [2109.07127](#).
4. Chu, X., Ilyas, I. F., Krishnan, S. & Wang, J. Data cleaning: Overview and emerging challenges. In *Proceedings of the 2016 International Conference on Management of Data*, 2201–2206 (2016).
5. Brodley, C. E. & Friedl, M. A. Identifying mislabeled training data. *J. artificial intelligence research* **11**, 131–167 (1999).
6. Smith, M. R. & Martinez, T. Improving classification accuracy by identifying and removing instances that should be misclassified. In *The 2011 International Joint Conference on Neural Networks*, 2690–2697 (IEEE, 2011).
7. Smith, M. R., Martinez, T. & Giraud-Carrier, C. The potential benefits of filtering versus hyper-parameter optimization. *arXiv preprint arXiv:1403.3342* (2014). [1403.3342](#).
8. Smith, M. R. & Martinez, T. An extensive evaluation of filtering misclassified instances in supervised classification tasks. *arXiv preprint arXiv:1312.3970* (2013). [1312.3970](#).
9. Zhu, X. & Wu, X. Class noise vs. attribute noise: A quantitative study. *Artif. intelligence review* **22**, 177–210 (2004).
10. Nettleton, D. F., Orriols-Puig, A. & Fornells, A. A study of the effect of different types of noise on the precision of supervised learning techniques. *Artif. intelligence review* **33**, 275–306 (2010).
11. Baptista, R. & Poloczek, M. Bayesian optimization of combinatorial structures. In *International Conference on Machine Learning*, 462–471 (PMLR, 2018).
12. Koshikawa, A. S., Ohzeki, M., Kadowaki, T. & Tanaka, K. Benchmark test of black-box optimization using d-wave quantum annealer. *J. Phys. Soc. Jpn.* **90**, 064001 (2021).
13. Koshikawa, A. S. *et al.* Combinatorial black-box optimization for vehicle design problem. *arXiv preprint arXiv:2110.00226* (2021). [2110.00226](#).
14. Doi, M., Nakao, Y., Tanaka, T., Sako, M. & Ohzeki, M. Exploration of new chemical materials using black-box optimization with the D-wave quantum annealer. *Front. Comput. Sci.* **5**, 1286226 (2023).
15. Morita, K., Nishikawa, Y. & Ohzeki, M. Random postprocessing for combinatorial Bayesian optimization. *J. Phys. Soc. Jpn.* **92**, 123801 (2023).
16. Kadowaki, T. & Nishimori, H. Quantum annealing in the transverse Ising model. *Phys. Rev. E* **58**, 5355–5363 (1998).
17. Farhi, E. *et al.* A quantum adiabatic evolution algorithm applied to random instances of an NP-complete problem. *Science* **292**, 472–475 (2001).
18. Johnson, M. W. *et al.* Quantum annealing with manufactured spins. *Nature* **473**, 194–198 (2011).
19. McGeoch, C. C. & Wang, C. Experimental evaluation of an adiabatic quantum system for combinatorial optimization. In *Proceedings of the ACM International Conference on Computing Frontiers*, 1–11 (2013).
20. Lucas, A. Ising formulations of many NP problems. *Front. physics* **2**, 5 (2014).
21. Zucca, A., Sadeghi, H., Mohseni, M. & Amin, M. H. Diversity metric for evaluation of quantum annealing. *arXiv preprint arXiv:2110.10196* (2021). [2110.10196](#).
22. Mohseni, M. *et al.* Sampling diverse near-optimal solutions via algorithmic quantum annealing. *Phys. Rev. E* **108**, 065303 (2023).
23. Carvalho, C. M., Polson, N. G. & Scott, J. G. Handling sparsity via the horseshoe. In *Artificial Intelligence and Statistics*, 73–80 (PMLR, 2009).

24. Bhattacharya, S., Khare, K. & Pal, S. Geometric ergodicity of Gibbs samplers for the Horseshoe and its regularized variants. *Electron. J. Stat.* **16**, 1–57 (2022).
25. Tibshirani, R. Regression shrinkage and selection via the lasso. *J. Royal Stat. Soc. Ser. B: Stat. Methodol.* **58**, 267–288 (1996).
26. OpenJij. <https://github.com/OpenJij/OpenJij> (2024).
27. D-Wave Neal. <https://github.com/dwavesystems/dwave-neal> (2024).
28. comparison\_of\_neal\_and\_openjij\_128.ipynb. <https://gist.github.com/tanemaki/79ac80803c1270a2650d9f4888486ce0> (2025).
29. DWaveCliqueSampler. <https://docs.ocean.dwavesys.com/projects/system/en/stable/reference/samplers.html#dwavecliquesampler>.
30. McGeoch, C. & Farre, P. *The D-Wave Advantage System: An Overview*. D-Wave Technical Report Series, 14-1049A-A (D-Wave Systems Inc., Burnaby, BC, 2020).

## Acknowledgements

We would like to extend our sincere gratitude to all participants of Quantum Infinity for You, The First Session with You, in Kumamoto (QI4U). In particular, we would like to thank Tadashi Kadowaki for guiding our research in the initial phase and Akira Sasao for organizing the event.

## Author contributions statement

M.O.\* conceptualized and designed the study, conducted numerical experiments, analyzed the results, and wrote and revised the manuscript. K.K. assisted with conceptualization and coding, and reviewed the manuscript. K.M. assisted with coding, wrote and revised the manuscript. M.O. assisted with conceptualization, wrote and revised the manuscript. All authors reviewed the results and approved the final version of the manuscript.

## Additional information

### Competing interests

The authors declare no competing interests.